Chemical Science

ROYAL SOCIETY OF CHEMISTRY

EDGE ARTICLE

View Article Online
View Journal | View Issue

Check for updates

Cite this: *Chem. Sci.*, 2021, **12**, 5315

All publication charges for this article have been paid for by the Royal Society of Chemistry

Received 24th January 2021
Accepted 25th February 2021

DOI: 10.1039/d1sc00440a

rsc.li/chemical-science

Selective adsorptive separation of cyclohexane over benzene using thienothiophene cages†

Yanjun Ding,[a] Lukman O. Alimi,[a] Basem Moosa,[a] Carine Maaliki,[b] Johan Jacquemin,[b] Feihe Huang[c] and Niveen M. Khashab*[a]

The selective separation of benzene (Bz) and cyclohexane (Cy) is one of the most challenging chemical separations in the petrochemical and oil industries. In this work, we report an environmentally friendly and energy saving approach to separate Cy over Bz using thienothiophene cages (ThT-cages) with adaptive porosity. Interestingly, cyclohexane was readily captured selectively from an equimolar benzene/cyclohexane mixture with a purity of 94%. This high selectivity arises from the C–H···S, C–H···π and C–H···N interactions between Cy and the thienothiophene ligand. Reversible transformation between the nonporous guest-free structure and the host–guest assembly, endows this system with excellent recyclability with minimal energy requirements.

Introduction

Energy-efficient separation of benzene derivatives with analogous structures and physical properties is regarded as one of the most critical separations that can change the world.[1] Specifically, the separation of benzene (Bz) and cyclohexane (Cy) is classified as an incredibly challenging task.[2,3] Bz has tremendous significance in the manufacturing of key chemicals while Cy is an important feedstock for varnishes, resins, and nylon fibers.[4] Cy is mainly obtained from the catalytic hydrogenation of Bz where it is significant to remove the unreacted Bz from the reactor's effluent stream for high-purity Cy.[5] However, traditional methods such as regular distillation are unable to separate Bz and Cy due to their comparable physical properties where there is a 0.6 K difference between their boiling points (bp for Bz = 353.25 K and Cy = 353.85 K).[6,7] The most common industrial methods for the separation of Bz/Cy mixtures are extractive and azeotropic distillations.[8–10] Nonetheless, these processes require complex operation and high energy, leading to high operating costs.

Exploiting molecular differences in terms of size and geometry, many efficient separation methods have been developed to separate Bz/Cy mixtures using membranes and porous materials.[4,11–13] Recently, adsorptive separation employing porous materials has attracted much attention due to its moderate energy demands, dependable recyclability and straight-forward synthetic techniques.[14–20] Among these porous materials, metal–organic frameworks (MOFs) have been experimentally investigated for the preferential uptake of Bz over Cy.[21–24] Earlier this year, Sue's and Huang's groups independently achieved the separation of Bz over Cy using nonporous adaptive crystals (NACs) based on pillararene macrocycles.[25,26] Jiang and co-workers realized the separation of the ternary mixture of Bz, Cy and cyclohexene through adsorptive separation using amide naphthotube solids.[27] All of these reports were focused on the separation of Bz over Cy or cyclohexene due to favourable non-covalent bonding such as π–π interactions of Bz with the aromatic rings of the porous platform. Compared to Bz,

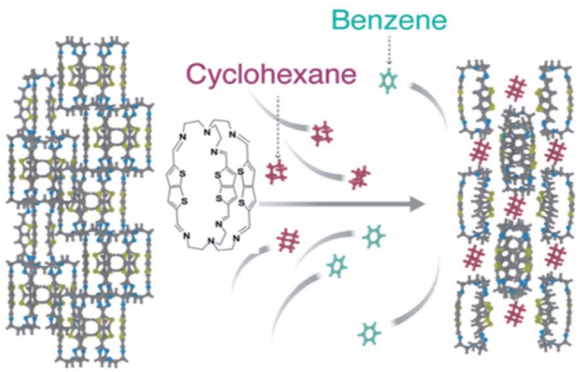

Scheme 1 Schematic illustration of the capture of Cy from a Bz/Cy mixture using ThT-cage crystals.

[a]*Smart Hybrid Materials (SHMs) Laboratory, Advanced Membranes and Porous Materials Center, King Abdullah University of Science and Technology (KAUST), Thuwal 23955-6900, Kingdom of Saudi Arabia. E-mail: niveen.khashab@kaust.edu.sa*
[b]*Laboratoire PCM2E, Université de Tours, Parc de Grandmont, 37200 Tours, France*
[c]*State Key Laboratory of Chemical Engineering, Center for Chemistry of High-Performance & Novel Materials, Department of Chemistry, Zhejiang University, Hangzhou 310027, P. R. China*

† Electronic supplementary information (ESI) available: Single crystal X-ray data, NMR, TGA, and PXRD results and crystal structures. Tables S2–S8 give the details of intermolecular interactions between hosts and guests. Table S9 shows the details of DFT calculations. CCDC 2058343–2058345. For ESI and crystallographic data in CIF or other electronic format see DOI: 10.1039/d1sc00440a

Open Access Article. Published on 25 February 2021. Downloaded on 1/24/2022 4:05:24 PM.
This article is licensed under a Creative Commons Attribution-NonCommercial 3.0 Unported Licence.

Open Access Article. Published on 25 February 2021. Downloaded on 1/24/2022 4:05:24 PM.
This article is licensed under a Creative Commons Attribution-NonCommercial 3.0 Unported Licence.

the conformation of Cy makes it hard for Cy molecules to diffuse into the cavities of porous materials. Nonetheless, Cy has abundant hydrogen atoms that can be preferably utilized for selective hydrogen bonding.

Most recently, easily scalable and processable organic cages with guest-adaptive porosity were successfully used in a wide range of adsorptive separations such xylene isomer separation.[28–39] Herein, we report an efficient method to successfully separate Cy from an equimolar Bz/Cy mixture by a thienothiophene organic cage (ThT-cage) with a selectivity of 94% and high recyclability (Scheme 1). The originally non-porous cages readily accommodate Cy over Bz molecules due to the favourable C–H···S, C–H···π and C–H···N interactions. To the best of our knowledge, this is the first example of adsorptive separation of Cy over Bz by using intricately designed organic cages that can selectively accommodate guest molecules on-demand.

Results and discussion

The ThT-cage was successfully synthesized by the one-step reaction of thieno[2,3-*b*]thiophene-2,5-dicarboxaldehyde and tris(2-aminoethyl)amine (Tren) in acetonitrile *via* an imine condensation reaction (Scheme S1†). ^{1}H and ^{13}C NMR spectra and mass spectra results indicated the formation of the ThT-cage as a pure product (Fig. S1 and S2†). ThT-cage crystals (ThT-cage 1) were recrystallized from chloroform and hexane, and then dried under vacuum at 80 °C for 24 h to obtain the activated crystalline adsorptive material (ThT-cage 1α). Single crystal X-ray diffraction (SCXRD) results confirmed the exact chemical structure of ThT-cage crystals (Table S1†) and further verified the successful synthesis of the ThT-cage. Thermogravimetric analysis (TGA) data supported that the solvent was completely removed from the activated ThT-cage 1 compared to the as-synthesized ThT-cage crystals, as shown in Fig. S3.† In the crystal structure of ThT-cage crystals (ThT-cage 1), there are chloroform molecules surrounding the neighbouring cage hosts through noncovalent interactions. Removing chloroform from the crystals yielded a new form of crystalline periodic packing. As shown in powder X-ray diffraction (PXRD), ThT-cage 1α maintained its crystallinity after losing the solvent (Fig. S4†). A nitrogen sorption experiment showed that ThT-cage 1 was nonporous, with a BET surface area of 8 m^2 g^{-1} (Fig. S5†).

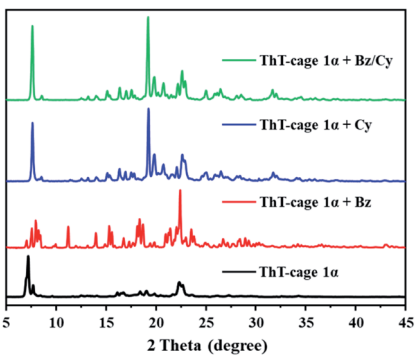

Fig. 1 Experimental PXRD patterns of ThT-cage 1α after being exposed to Bz/Cy for 24 h.

Powder X-ray diffraction (PXRD) and ^{1}H NMR experiments were carried out to investigate the adsorption capacity of Bz and Cy in ThT-cage 1α. Firstly, solid-vapor sorption experiments were performed with ThT-cage 1α towards Bz/Cy. As demonstrated in Fig. 1, the powder X-ray diffraction (PXRD) patterns of ThT-cage 1α presented changes after being exposed to Bz or Cy vapor at room temperature, consequently supporting the formation of new structures of ThT-cage 1α after adsorption of guest molecules. Significantly, the PXRD results revealed a preferred uptake of Cy over Bz (Fig. 1). The ^{1}H NMR results of ThT-cage 1α after adsorption of Bz or Cy vapor demonstrated the adsorption capacity of ThT-cage 1α and confirmed a selective adsorption of Cy over Bz with high selectivity (Fig. S6–S8†). ThT-cage 1α is insoluble in Bz or Cy, which makes the adsorption process quite straightforward in solution without the need to dissolve ThT-cage 1α into microdroplets and then recrystallize it with the intercalated guest.

To investigate the dynamics of the adsorption process, time-dependent solid-vapor sorption experiments were carried out *via* ^{1}H NMR spectroscopy and powder X-ray diffraction (PXRD). ThT-cage 1α took a relatively longer time to host the guest molecules with a single-component adsorption of Bz or Cy vapor (Fig. S9†) while the adsorption of the Bz/Cy mixture showed a fast-structural change in less time (*ca.* 2 h). At the saturation adsorption point, *ca.* 1.4 Bz molecules were adsorbed on average by one cage, and *ca.* 0.9 Cy molecules were captured on average by one cage (Fig. S10†). Time-dependent solid-liquid sorption experiments were also conducted to check whether ThT-cage 1α could work in solution. PXRD patterns indicated that ThT-cage 1α still maintained its selectivity towards Cy in the presence of Bz with improved adsorption dynamics (Fig. S11†).

To better understand the mechanism of the selective adsorption of Cy over Bz, ThT-cage 1 was used to obtain single crystals with benzene (ThT-cage 2) and cyclohexane (ThT-cage 3) guest molecules, respectively. The single crystals of ThT-cage 2 were easily grown by the slow cooling of a hot benzene solution to room temperature, giving colorless block crystals (Table S1†). Liquid diffusion of cyclohexane into a chloroform solution of ThT-cage 1 at room temperature provided needle-like colorless crystals of ThT-cage 3 (Table S1†). In the crystal structure of ThT-cage 2, Bz guest molecules were not located inside the cage but rather in the voids of the cage packing structure (Fig. 2a and S12†). The ratio of Bz/cage was 1.5 : 1 (Fig. S13a†). As exhibited in the crystal packing structure of ThT-cage 2, there were two types of benzene guest molecules. One molecule showed both weak C–H···S and C–H···π intermolecular interactions with the neighbouring cages, and the other one only displayed weak C–H···S intermolecular interactions (Fig. 2b, Tables S2 and S3†). The cages also presented weak noncovalent interactions between each other (Fig. 2c, d, Tables S4 and S5†). Unlike ThT-cage 2, ThT-cage 3 crystal packing gave a ratio of 1 : 1 between the Cy guest molecules and the cages (Fig. S13b†). All Cy guests were intercalated within the voids of the cage packing structure (Fig. 3a and S14†). Cy molecules had strong intermolecular interactions with the neighbouring cages *via* the C–H···S and C–H···π bonding (Fig. 3b, Tables S6 and S7†). Similar to ThT-cage 2, ThT-cage 3 showed noncovalent interactions between the

© 2021 The Author(s). Published by the Royal Society of Chemistry

Open Access Article. Published on 25 February 2021. Downloaded on 1/24/2022 4:05:24 PM.
This article is licensed under a Creative Commons Attribution-NonCommercial 3.0 Unported Licence.

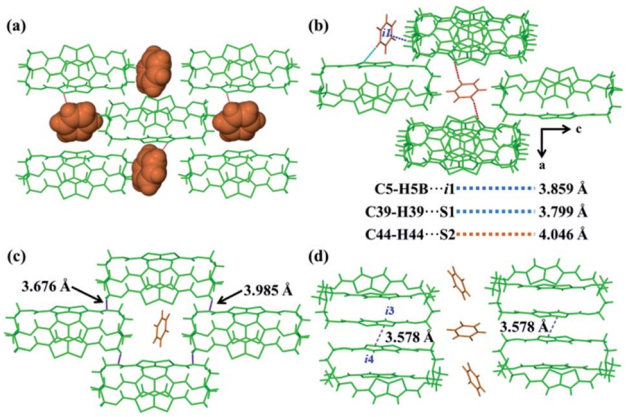

Fig. 2 Single-crystal structure of ThT-cage 2. (a) Perspective showing Bz (space filed) molecules between ThT-cages. (b) Illustration of the C–H···π and C–H···S interactions between Bz and ThT-cage molecules. (c and d) Host–host C–H···N and π···π interactions between ThT-cages.

packed cages (Fig. 3c and Table S8†). Compared to the intermolecular host–guest interactions in ThT-cage 2, noncovalent interactions were much stronger between Cy guests and ThT-cage 3 (Fig. 2b and 3b). Therefore, the selective adsorption of Cy over Bz can be attributed to the formation of a highly stable crystal structure. Additionally, thermogravimetric analysis (TGA) of ThT-cage 2 and ThT-cage 3 crystals confirmed the respective loss of *ca.* 1.5 Bz molecules and *ca.* 1.0 Cy molecules on average, respectively, per cage. It also displayed a high binding energy for the removal of Cy guests, which further supports the high selectivity of ThT-cage 1α for Cy (Fig. S15†). DFT calculations were then performed to support our findings (Table S9†) which showed that Cy is the preferred guest with a lower G°, 298 K (−8.350 kcal mol^{-1}), compared to Bz (−5.159 kcal mol^{-1}).

Based on this analysis, we hypothesize that Bz and Cy molecules have a synergistic effect to accelerate structural transformation.[40] Thus, the planar Bz molecules can open the space between the cages to facilitate the adsorption process of Cy molecules, which can tightly occupy this space due to their

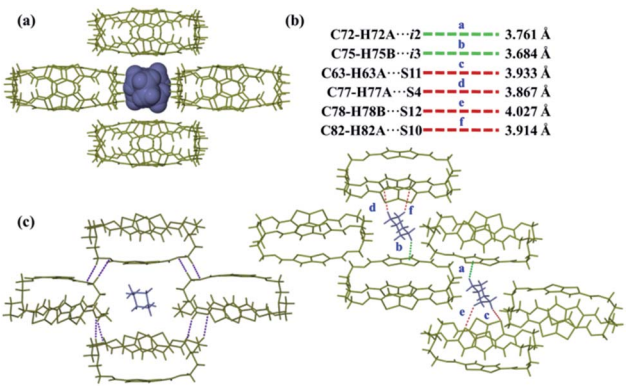

Fig. 3 Single-crystal structure of ThT-cage 3. (a) Perspective showing a Cy (space filed) molecule between ThT-cages. (b) Illustration of the C–H···π and C–H···S interactions between Cy and ThT-cage molecules. (c) Host–host C–H···N interactions between ThT-cages.

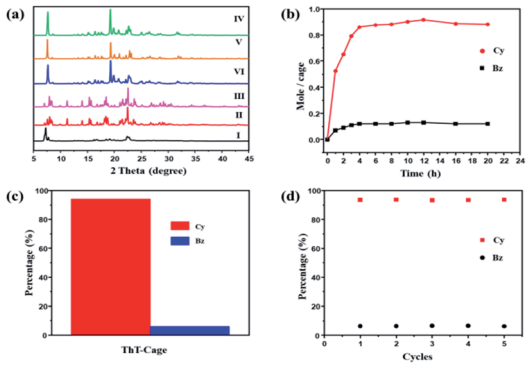

Fig. 4 (a) Experimental PXRD patterns of ThT-cage 1α: (I) blank; (II) after adsorption of Bz vapor; (III) simulated from the single-crystal structure of ThT-cage 2; (IV) after adsorption of Cy vapor; (V) simulated from the single-crystal structure of ThT-cage 3; (VI) after adsorption of the Bz/Cy mixture vapor. (b) Time-dependent solid-vapor sorption plot for the equimolar Bz/Cy mixture. (c) Relative uptake of Bz and Cy adsorbed by ThT-cage 1α for over 12 h. (d) Relative uptake of the equimolar Bz/Cy mixture for 5 cycles.

stronger interactions, as showcased in SCXRD. The powder X-ray diffraction (PXRD) patterns of ThT-cage 1α after uptake of Bz/Cy were consistent with the simulated ones from the crystal structure of ThT-cage 2 and ThT-cage 3 (Fig. 4a). At the saturation adsorption point, one molecule of the cage can capture and recover 0.89 molecule Cy on average from the equimolar Bz/Cy mixture based on ^{1}H NMR integration (Fig. 4b). Differential scanning calorimetry (DSC) not only showed the loss of solvent (Cy or Bz) at high temperature, but presented the selectivity of Cy uptake from the Cy/Bz mixture (Fig. S16†). Gas chromatography results confirmed the high percentage of Cy (94.7%) adsorbed by the ThT-cage 1α (Fig. 4c and S17†).

For industrial production, the recycling capacity and stability are vital criteria for assessing an adsorbent. ThT-cage 1α after adsorption could be readily regenerated upon heating at 100 °C under vacuum to release the adsorbed guest molecules, while the released Cy could be collected *via* a condensation setup. The re-activated porous material was able to selectively capture Cy from Bz/Cy mixtures with minor loss of performance after 5 cycles (Fig. 4d and S18†). In addition, the stability of ThT-cage 1α was tested in water. Although, the stability of imine bonds in aqueous solutions is still an enigma to researchers, ThT-cage 1α remained stable in an aqueous solution for a week with no signs of decomposition (Fig. S19†). We envisage that the strong intermolecular non-covalent interactions within the crystal packing provides the cage system with improved stability. Compared to other selective adsorbents for the separation of Bz and Cy (Table S10†), the ThT-cage showed superior performance in the vapor phase and in solution with Cy selectivity.

Conclusions

We have successfully developed a new method to separate Cy from an equimolar Bz/Cy mixture using an easily scalable ThT-cage with a selectivity of 94%. The selective adsorption behaviour originates from the strong intermolecular interactions

© 2021 The Author(s). Published by the Royal Society of Chemistry

Open Access Article. Published on 25 February 2021. Downloaded on 1/24/2022 4:05:24 PM. This article is licensed under a Creative Commons Attribution-NonCommercial 3.0 Unported Licence.

between Cy and ThT-cages, forming a highly stable crystal structure *via* hydrogen bonding. Moreover, reversible transformation between the nonporous guest-free structure and the adsorptive guest-containing assembly made our system highly recyclable. The ease of preparation, high separation efficiency, stability and outstanding recycling performance of ThT-cages endows this class of materials with substantial prospects to be used as an energy-efficient molecular sieving system in the chemical and petrochemical industries.

Conflicts of interest

There are no conflicts to declare.

Acknowledgements

This work was supported by the Office of Sponsored Research-CRG 4 at King Abdullah University of Science and Technology (KAUST).

References

1 D. S. Sholl and R. P. Lively, *Nature*, 2016, **532**, 435–437.
2 B. Manna, S. Mukherjee, A. V. Desai, S. Sharma, R. Krishna and S. K. Ghosh, *Chem. Commun.*, 2015, **51**, 15386–15389.
3 Y. Yang, P. Bai and X. Guo, *Ind. Eng. Chem. Res.*, 2017, **56**, 14725–14753.
4 J. G. Villaluenga and A. Tabe-Mohammadi, *J. Membr. Sci.*, 2000, **169**, 159–174.
5 A. Stanislaus and B. H. Cooper, *Catal. Rev.: Sci. Eng.*, 1994, **36**, 75–123.
6 C. X. Ren, L. X. Cai, C. Chen, B. Tan, Y. J. Zhang and J. Zhang, *J. Mater. Chem. A*, 2014, **2**, 9015–9019.
7 J. P. Zhang and X. M. Chen, *J. Am. Chem. Soc.*, 2008, **130**, 6010–6017.
8 P. Navarro, A. Ovejero-Pérez, M. Ayuso, N. Delgado-Mellado, M. Larriba, J. García and F. Rodríguez, *J. Mol. Liq.*, 2019, **289**, 111120.
9 J. Qin, Q. Ye, X. Xiong and N. Li, *Ind. Eng. Chem. Res.*, 2013, **52**, 10754–10766.
10 A. Vega, F. Díez, R. Esteban and J. Coca, *Ind. Eng. Chem. Res.*, 1997, **36**, 803–807.
11 M. J. Emparan-Legaspi, J. Gonzalez, G. Gonzalez-Carrillo, S. G. Ceballos-Magaña, J. Canales-Vazquez, I. A. Aguayo-Villarreal and R. Muñiz-Valencia, *Microporous Mesoporous Mater.*, 2020, **294**, 109942.
12 C. González-Galán, A. Luna-Triguero, J. M. Vicent-Luna, A. P. Zaderenko, A. Sławek, R. Sánchez-de-Armas and S. Calero, *Chem. Eng. J.*, 2020, **398**, 125678.
13 H. Tan, Q. Chen, T. Chen and H. Liu, *ACS Appl. Mater. Interfaces*, 2018, **10**, 32717–32725.
14 W. Bury, A. M. Walczak, M. K. Leszczyński and J. A. Navarro, *J. Am. Chem. Soc.*, 2018, **140**, 15031–15037.
15 S. Shimomura, S. Horike, R. Matsuda and S. Kitagawa, *J. Am. Chem. Soc.*, 2007, **129**, 10990–10991.
16 Y. Wang, K. Xu, B. Li, L. Cui, J. Li, X. Jia, H. Zhao, J. Fang and C. Li, *Angew. Chem., Int. Ed.*, 2019, **58**, 10281–10284.
17 J. R. Wu, B. Li and Y. W. Yang, *Angew. Chem., Int. Ed.*, 2020, **59**, 2251–2255.
18 J. R. Wu and Y. W. Yang, *Angew. Chem., Int. Ed.*, 2021, **60**, 1690–1701.
19 J. R. Wu and Y. W. Yang, *J. Am. Chem. Soc.*, 2019, **141**, 12280–12287.
20 J. R. Wu and Y. W. Yang, *Small*, 2020, **16**, 2003490.
21 A. Karmakar, A. V. Desai, B. Manna, B. Joarder and S. K. Ghosh, *Chem.–Eur. J.*, 2015, **21**, 7071–7076.
22 A. A. Lysova, D. G. Samsonenko, P. V. Dorovatovskii, V. A. Lazarenko, V. N. Khrustalev, K. A. Kovalenko, D. N. Dybtsev and V. P. Fedin, *J. Am. Chem. Soc.*, 2019, **141**, 17260–17269.
23 L. K. Macreadie, E. J. Mensforth, R. Babarao, K. Konstas, S. G. Telfer, C. M. Doherty, J. Tsanaktsidis, S. R. Batten and M. R. Hill, *J. Am. Chem. Soc.*, 2019, **141**, 3828–3832.
24 S. Mukherjee, B. Manna, A. V. Desai, Y. Yin, R. Krishna, R. Babarao and S. K. Ghosh, *Chem. Commun.*, 2016, **52**, 8215–8218.
25 W. Yang, K. Samanta, X. Wan, T. U. Thikekar, Y. Chao, S. Li, K. Du, J. Xu, Y. Gao, H. Zuihof and A. C. H. Sue, *Angew. Chem., Int. Ed.*, 2020, **59**, 3994–3999.
26 J. Zhou, G. Yu, Q. Li, M. Wang and F. Huang, *J. Am. Chem. Soc.*, 2020, **142**, 2228–2232.
27 H. Yao, Y. M. Wang, M. Quan, M. U. Farooq, L. P. Yang and W. Jiang, *Angew. Chem., Int. Ed.*, 2020, **59**, 19945–19950.
28 M. Mastalerz, *Acc. Chem. Res.*, 2018, **51**, 2411–2422.
29 M. A. Little and A. I. Cooper, *Adv. Funct. Mater.*, 2020, 1909842.
30 B. A. Moosa, L. O. Alimi, A. Shkurenko, A. Fakim, P. M. Bhatt, G. Zhang, M. Eddaoudi and N. M. Khashab, *Angew. Chem., Int. Ed.*, 2020, **59**, 21367–21371.
31 Y. Lei, Q. Chen, P. Liu, L. Wang, H. Wang, B. Li, X. Lu, Z. Chen, Y. Pan, F. Huang and H. Li, *Angew. Chem., Int. Ed.*, 2021, **60**, 4705–4711.
32 G. Zhang, B. Hua, A. Dey, M. Ghosh, B. A. Moosa and N. M. Khashab, *Acc. Chem. Res.*, 2021, **54**, 155–168.
33 Z. Wang, N. Sikdar, S. Q. Wang, X. Li, M. Yu, X. H. Bu, Z. Chang, X. Zou, Y. Chen, P. Cheng and K. Yu, *J. Am. Chem. Soc.*, 2019, **141**, 9408–9414.
34 E. Berardo, L. Turcani, M. Miklitz and K. E. Jelfs, *Chem. Sci.*, 2018, **9**, 8513–8527.
35 S. Jiang, Y. Du, M. Marcello, E. W. Corcoran, D. C. Calabro, S. Y. Chong, L. J. Chen, R. Clowes, T. Hasell and A. I. Cooper, *Angew. Chem., Int. Ed.*, 2018, **57**, 11228–11232.
36 S. Komulainen, J. Roukala, V. V. Zhivonitko, M. A. Javed, L. Chen, D. Holden, T. Hasell, A. Cooper, P. Lantto and V. V. Telkki, *Chem. Sci.*, 2017, **8**, 5721–5727.
37 T. Hasell, M. Miklitz, A. Stephenson, M. A. Little, S. Y. Chong, R. Clowes, L. Chen, D. Holden, G. A. Tribello, K. E. Jelfs and A. I. Cooper, *J. Am. Chem. Soc.*, 2016, **138**, 1653–1659.
38 I. Cooper, *Angew. Chem., Int. Ed.*, 2011, **50**, 996–998.
39 Y. Jin, B. A. Voss, R. D. Noble and W. Zhang, *Angew. Chem., Int. Ed.*, 2010, **49**, 6348–6351.
40 W. Hao, X. Chen and S. Li, *J. Phys. Chem. C*, 2016, **120**, 28448.

© 2021 The Author(s). Published by the Royal Society of Chemistry